



REGULAR ARTICLE

Synthesis of High Electrical Conductivity of Superconductor NiS Thin Films

A. Sbaihi^{1,2,3}, S. Benramache^{2,*} ✉, C. Benbrika³

¹ Laboratoire des Matériaux Semi-Conducteurs et Métalliques, University of Biskra 07000, Algeria

² Laboratoire des Matériaux, des Énergies et de l'Environnement, University of Biskra 07000, Algeria

³ Material Sciences Department, Faculty of Science, University of Biskra 07000, Algeria

(Received 12 December 2023; revised manuscript received 20 February 2024; published online 28 February 2024)

In this work, we prepared and studied the physical properties of nickel sulfide (NiS) nanostructure thin films, which were deposited on heated glasses substrates ($T = 250^\circ\text{C}$) using the spray pyrolysis technique (SPT) using different Precursor concentrations of these two solution sources: nickel nitrates hexahydrate $\{(\text{Ni}(\text{NO}_3)_2 \cdot 6\text{H}_2\text{O}) = \text{X}\}$ and thiourea $\{(\text{CS}(\text{NH}_2)_2) = \text{Y}\}$: $\{30\% [\text{X}], 70\% [\text{Y}]\}$, $\{33\% [\text{X}], 67\% [\text{Y}]\}$ & $\{37\% [\text{X}], 63\% [\text{Y}]\}$ with fixing the other remaining experimental conditions, and this is to understand more the role of the Precursor concentrations of the solutions on the physical properties of nickel sulfide thin films. The results of X-ray diffraction (DRX) analysis showed that all nickel sulfide (NiS) thin films samples are polycrystalline in a hexagonal phase and have a preferred orientation of (010). The Crystallite size (D) was estimated by The Debye-Scherrer's relation, ranging from 9.915 nm to 22.148 nm. The emergence of the Ni-S bond corresponding to the frequency 668.563 cm^{-1} was confirmed by FTIR analysis. On the other hand, the energy of the band gaps varies for samples from 0.87, 0.88 to 0.92 eV. Finally, the Sheet resistance (R_{sh}) was measured using the four-point method, which it used to determine the conductivity of the samples.

Keywords: NiS, Spray pyrolysis, Thin film, X-Ray diffraction.

DOI: [10.21272/jnep.16\(1\).01022](https://doi.org/10.21272/jnep.16(1).01022)

PACS number: 74.25.fc

1. INTRODUCTION

Recent scientific papers proved that nanostructured transition metal sulphides (TMS) have a great importance in the scientific field, providing many applications because of their distinctive properties of high superconductivity, good electrochemical stability, their environmentally friendly nature and their low cost [1,2].

Nickel sulfide is a transition metal of the chalcogen elements, it is considered one of the most attracting and interesting material due to its high electron transfer potential, good reflectivity in the infrared range, ease of production and low toxicity [3]. What makes it even more interesting is the presence of different phases and stoichiometric measurements such as NiS, Ni₃S₂, Ni₃S₄, Ni₇S₁₀ and their different forms that make this substance an important and challenging material for scientists. Generally, NiS exists in two phases, one hexagonal and the other rhombohedral [4, 5]. In both of these phases, NiS shows excellent capacity performance, and high oxidation activity, which can satisfy the growing need for energy storage systems [6].

Nickel sulfide (NiS) is a p-types semiconductor; it is the most effective electrochemically active material due to the variety of its applications such as lithium ion batteries, supercapacitors, photocatalytic H₂ generation and solar cells [7]. Many different methods have been used to deposit NiS thin films such as: spray pyrolysis [8]. Chemical bath deposition (CBD) [9] hydrothermal [10] successive ion layer desorption and reaction (SILAR) [11] thermal evaporation, [12]

Electrode position, [13] and Sol-Gel [14].

In this work, we have deposited of NiS thin film on glass substrates at different Precursor concentrations by spray pyrolysis technique. On the other hand, we have studied the structural, optical and electrical properties using the following devices: DRX, FTIR, UV-Visible & 4pt. Finally, we discussed and analyzed the obtained results, hoping for more research in the future.

2. EXPERIMENTAL PART

2.1 Preparation of (NiS) Thin Films

For the deposition of nickel sulfide NiS thin films by spray-pyrolysis method, We prepared a solution consisting of nickel nitrates hexahydrate $\{(\text{Ni}(\text{NO}_3)_2 \cdot 6\text{H}_2\text{O}) = \text{X}\}$ and thiourea $\{(\text{CS}(\text{NH}_2)_2) = \text{Y}\}$ as a source of nickel Ni and sulfur S respectively, their molar concentration is $(X\%[\text{Ni}], Y\%[\text{S}]; [C_{\text{Tot}} = 0.15 \text{ mol/l}])$ (see Fig. 1 and Table 1). Dissolved in a volume of 50 ml of distilled water, the mixture is stirred for an hour and a half (1 h 30 min) at a temperature of 60°C leading to the formation of a clear green and homogeneous solution. On the other hand, glass substrates with dimensions of $7.5 \text{ cm} / 2.6 \text{ cm}$ were washed well using water and soap, and then placed in Ethanol for 5 minutes; we repeated the process with Acetone. The experimental set-up was equipped by fixing the distance between the substrate and the spray nozzle at $d = 23 \text{ cm}$, the deposition process is carried out at a temperature of $T = 250^\circ\text{C}$ (see Fig. 2 and 3).

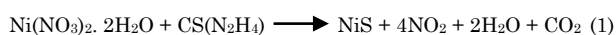
* Correspondence e-mail: benramache.sai@gmail.com



Table 1 – Experimental parameters

| Condition | Values |
|-----------------------|--|
| S1 | 30% [X].70% [Y] |
| S2 | 37% [X].63% [Y] |
| S3 | 33% [X].67% [Y] |
| Substrate temperature | $T = 250\text{ }^{\circ}\text{C}$ |
| Volume | $V = 50\text{ ml}$ |
| Deposition time | 10 min |
| Distance | $d = 23\text{ cm}$ |
| Flow rate of solution | 2 ml/min |
| The glass substrates | (CAT.NO.7101) microscope glass slide in size of $(7.5 \times 2.6)\text{ cm}$. |

The reaction takes place according to the following equation:



2.2 Cracterization Techniques

The X-Ray diffraction spectra was obtained by a (DRX Malvern Pnmanalytical Empeyrean) system, under $\text{CuK}\alpha$ radiation $\lambda = 1.5406\text{ \AA}$ in the range of $(20\text{-}80^{\circ})$ this is in order to study the structural properties of nickel sulfide thin films. Infra-Red Spectrometer, type (Perkinelmer Spectrum Two) was used in the frequency range of $400\text{-}4000\text{ cm}^{-1}$ to study the chemical bonding properties of the prepared films. As for the optical properties, they were studied using an UV-Visible spectrophotometer (Perkinelmer Lambda 35) in a wavelength range $(200\text{-}1200\text{ nm})$, the four-point method was used for the electrical properties measurements.

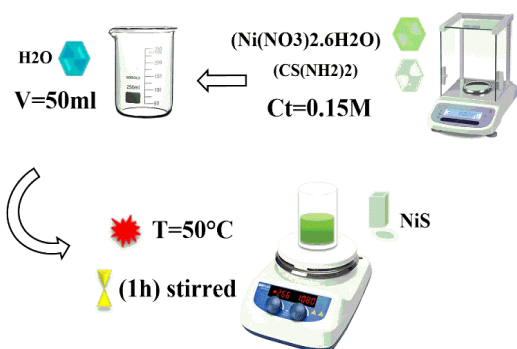


Fig. 1 – Steps for preparing a nickel sulfide solution

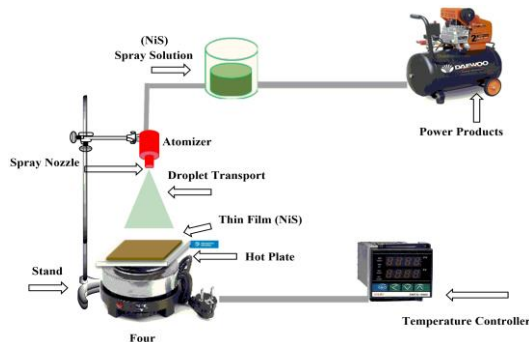


Fig. 2 – Illustration of a sample spray pyrolysis method

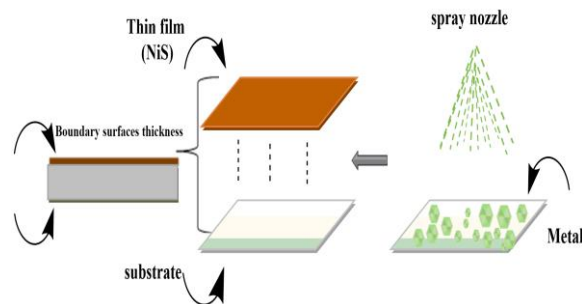


Fig. 3 – A schematic diagrams showing the phase of ion deposition of nickel sulfide thin films

In order to estimate the film thickness we used the weighing method, according to equation [15]:

$$t = \frac{\Delta m}{\rho s} \quad (2)$$

where t is the film thickness, m the mass deposited onto a substrate, s the area of the film and ρ is the density of NiS (5.50 g/cm^3).

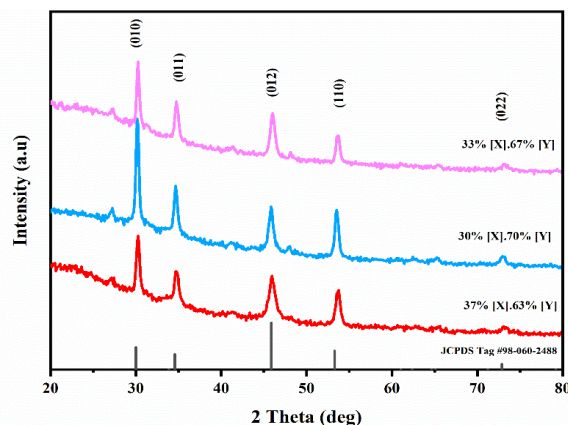


Fig. 4 – X-Ray patterns of NiS thin films prepared at different precursor concentrations

3. RESULTS AND DISCUSSION

3.1 X-ray Diffraction Analysis

The structural properties of nickel sulfide thin films were studied using X-ray diffraction diffractograms (DRX), where the Fig. 4 shows the X-ray diffraction spectra of nickel sulfide (NiS) thin films deposited on glass substrates using the spray pyrolysis technique (SPT) at a temperature of $250\text{ }^{\circ}\text{C}$. Fig. 4 shows that polycrystalline films with hexagonal structure are part of the $P6_3/mmc$ space group of preferred orientation (010) (JCPDS Tag # 98-060-2488), and on the other hand we observe diffraction peaks with orientation, (011), (101), (012), (110) and (022) respectively, according to the ASTAM data sheet. Using these diffractograms we can determine a lot of physical parameters such as the crystallite size, the dislocation density and the micro strain. The value of the Bragg angle 2θ corresponding to preferred orientation is determined as shown in the table below:

d_{hkl} represents the inter-plans distance, calculated using Bragg's law [16]:

$$2d_{hkl} \sin \theta = n\lambda \quad (3)$$

The hexagonal cell parameters (a , b and c) of nickel sulfide thin film are determined using the following equation [17]:

$$\frac{1}{d_{hkl}} = \frac{4}{3} \left(\frac{h^2 + k^2 + hk}{a^2} \right) + \frac{l^2}{c^2} \quad (4)$$

The unit cell V is calculated using the following Law [16]:

$$V = abc \sin(60^\circ) \quad (5)$$

The Debye-Scherrer's equation was used to calculate the crystallite size [18]:

$$D_{hkl} = \frac{k\lambda}{\beta \cos \theta} \quad (6)$$

where: β (rad) is full width at half-maximum FWHM, λ is the wavelength of X-ray ($\lambda = 1.5406$ Å), k is a constant ($k = 0.89$).

An increase in the crystallites size (D) was observed in the {30% [X].70% [Y]} sample compared to samples {33% [X].67% [Y]} and {37% [X].63% [Y]}. Through these results it is possible to explain the increase in the average crystallites size. It is because the small crystallites are consumed during the crystallization process, while the dislocations gain more energy and exhibits greater mobility, these activated dislocations separate toward the grains boundaries and are neutralized as the crystallization of the film proceeds [6].

δ_{hkl} represents The Dislocation density, it is calculated using the following relation [19]:

$$\delta_{hkl} = \frac{1}{D_{hkl}} \quad (7)$$

The Micro-Strain (ϵ) is determined by using the following Stokes-Wilson formula [20]:

$$\epsilon_{hkl} = \frac{\beta}{4 \tan \theta} \quad (8)$$

The increase in the crystallites size corresponds to a decrease in lattice defects, and this results in a decrease in internal stress and dislocation intensity [21] as shown in the following Table 2 and Fig. 5.

Table 2 – The crystallites size (D_{010}), Micro-stress (ϵ_{010}) and the dislocation density (δ_{10}) values of NiS thin films

| Precursor concentration | 37% [X].63% [Y] | 30% [X].70% [Y] | 33% [X].67% [Y] |
|---------------------------------|-----------------|-----------------|-----------------|
| D_{010} (nm) | 17.067 | 22.148 | 18.648 |
| δ_{010} | 3.432 | 2.038 | 2.875 |
| $\epsilon_{010} \times 10^{-3}$ | 7.786 | 6.013 | 6.642 |

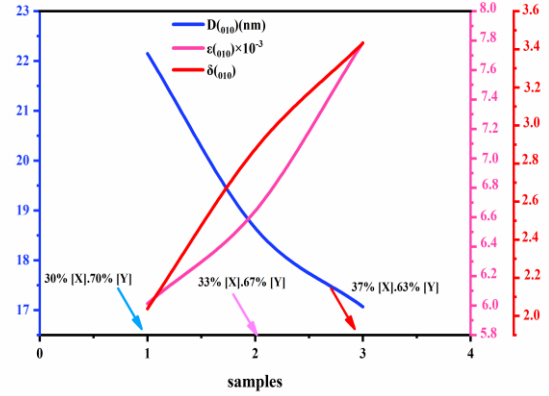


Fig. 5 – Variations of the crystallites size (D_{010}), Microstress (ϵ_{010}) and the dislocation density (δ_{10}) of NiS thin films as function of precursor concentration prepared at 250 °C

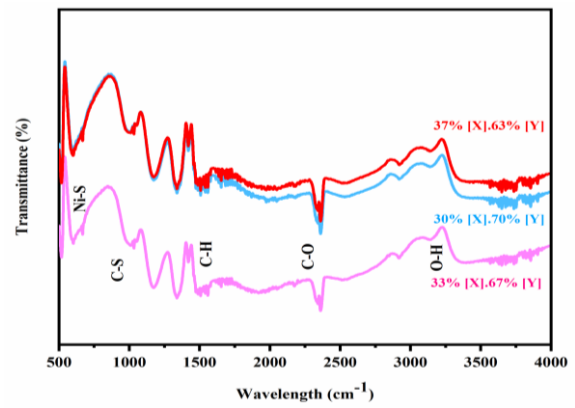


Fig. 6 – FTIR spectrum of nickel sulfide prepared at different Precursor

Table 3 – Association type and corresponding frequency

| Vibrations | The band | Reference |
|-----------------------|----------|------------|
| 626 cm^{-1} | Ni-S | [2-21] |
| 1092 cm^{-1} | C-S | [2-22-23] |
| 1483 cm^{-1} | C-H | [2] |
| 3275 cm^{-1} | O-H | [24-25-26] |
| 2375 cm^{-1} | C=O=O | [27] |

3.2 FTIR Analysis

The Fourier transforms Infra-Red spectroscopy (FTIR) results are provided for the nickel sulfide (NiS) thin films. These films were prepared by treating changes in the precursor concentrations of sulfur (S) and nickel (Ni) sources using the spray pyrolysis technique (SPT), as shown in Fig. 6. The FTIR results were obtained by scanning the sample in the wavelength range of (400 cm^{-1} to 4000 cm^{-1}). The locations of vibration sites in the infrared spectrum were used to observe the types of chemical bonds, and each vibration corresponding to a specific bond was identified. The summarized results of the study are presented in the Table 3.

3.3 UV-Vis Studies

The curve shown in Fig. 7 represents absorption spectra of nickel sulfide (NiS) thin films at a temperature of 250 °C by spray pyrolysis technique (SPT), the

absorption edge of all of (NiS) thin films is observed at 400 nm. The higher the wavelength is the lower the absorption becomes. The highest optical absorption ratio is observed for thin films deposited at positions {33% [X].67% [Y]} and {37% [X].63% [Y]} compared to the deposited membrane at {30% [X].70% [Y]}. This could be explained by the differences associated with the morphology and crystalline nature of the prepared films.

The optical band gap E_g of nickel sulfide (NiS) thin films deposited at 250 °C is associated with the point of intersection of the linear line with the photon energy $h\nu$, $A = 0$ as shown in Fig. 8.

The optical band gap energy E_g of NiS thin films, as presented in Table 4, was derived from the transmission spectra through the utilization of the following relations [28].

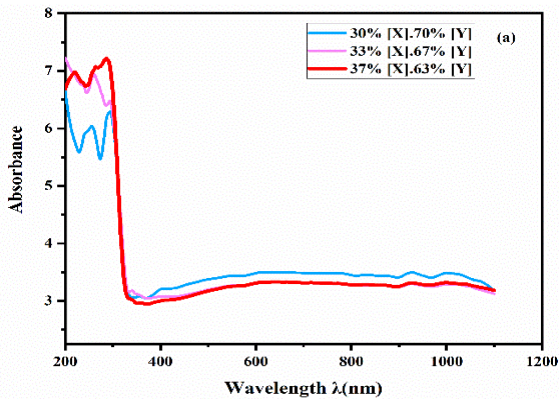


Fig. 7 – UV-Vis absorption spectra of the thin films of NiS at different precursor concentrations

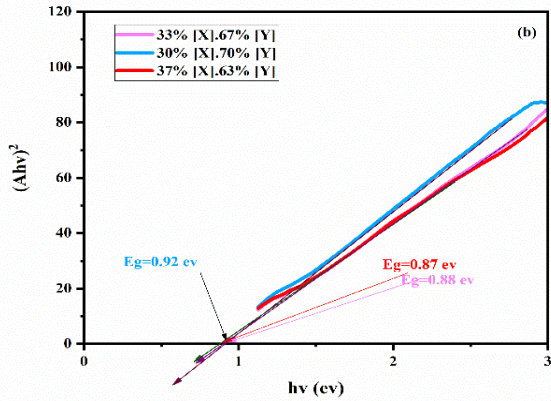


Fig. 8 – The Tauc plot for NiS thin films using different changes in the precursor concentrations sources

$$A = at = -LnT \quad (9)$$

$$(Ahv)^2 = B(hv - E_g) \quad (10)$$

where: A is the absorbance, d is the film thickness, T is the transmittance spectra of thin films a is the absorption coefficient values, B is a constant, $h\nu$ is the photon energy and E_g is the band gap energy. On the other hand, we can determine the Urbach energy through the following equation [29]:

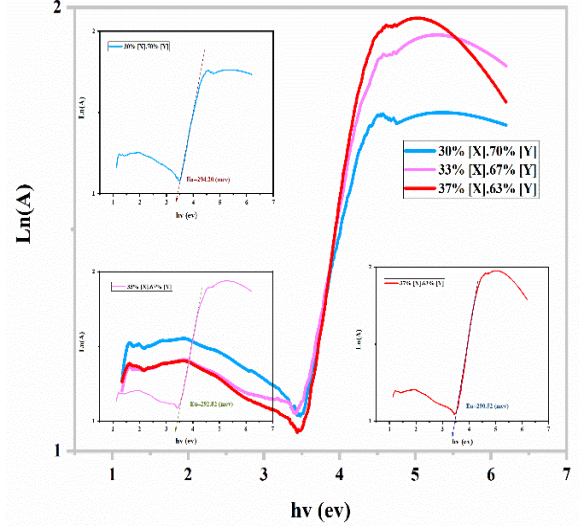


Fig. 9 – Determination of Urbach energy (E_u)

$$A = A_0 \exp\left(\frac{h\nu}{E_u}\right) \quad (11)$$

where: A_0 is a constant and E_u is the Urbach Energy, by plotting $Ln(A)$ in terms of $h\nu$, we can ascertain the value of E_g as the reciprocal of the linear tangent that intersects the photon energy at $x = 0$ as shown in Fig. 10 and Table 4. We notice a difference in the energy values of the gaps from 0.92, 0.88 and 0.87 eV for the samples {30% [X].70% [Y]}, {33% [X].67% [Y]} and {37% [X].63% [Y]} respectively, this is due to a difference in the ratio of nickel with sulfur, which results in a difference and change in the energy of the gaps and the density of states for the conduction and valence bands [30].

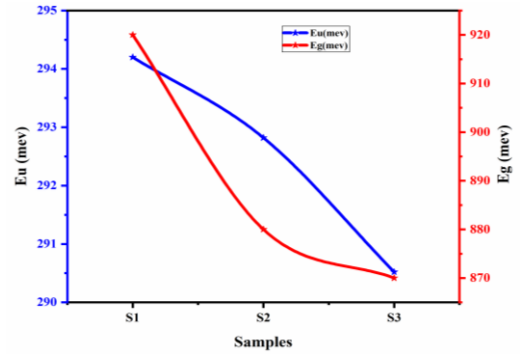


Fig. 10 – Variation of the Urbach energy E_u & band gap energy E_g of NiS thin films at three different samples

Table 4 – Band gap energy and Urbach energy for nickel sulfide NiS thin film samples

| Samples | E_g eV | E_u meV |
|-----------------|----------|-----------|
| 30% [X].70% [Y] | 0.92 | 294.20 |
| 33% [X].67% [Y] | 0.88 | 292.82 |
| 37% [X].63% [Y] | 0.87 | 290.52 |

3.4 Electrical Properties

The electrical properties of nickel sulfide thin films were studied by Four-point method at a temperature of 250°C, Fig. 11 shows the variation of voltage with cur-

rent, it also represents the electrical resistivity variation of nickel sulfide thin films, the voltage changed linearly with the increase of current in the range of 0 – 100 mA. The voltage value increases with the decrease in the sulfur concentration in the {30% [X].70% [Y]} sample compared to samples {33% [X].67 % [Y]} and {37% [X].63%[Y]}, on the other hand, the best resistance was measured in the {30% [X].70%[Y]}sample with a value of 5.304 Ω , and this indicates that it has good electrical conductivity with a value of $2.43 \cdot 10^3$ S/cm compared to samples {33% [X].67 % [Y]} and {37% [X].63% [Y]}. The electrical conductivity (σ) of the nickel sulfide thin films is calculated according to the relation (12) and we have summarized the results as shown in Fig. 12, which shows the thickness variation, resistivity and electrical conductivity of the nickel sulfide thin films from the above, we can see that [31].

$$R_{sh} = \frac{\pi}{Ln2} \frac{V}{I} \quad (12)$$

$$\sigma = \frac{1}{\rho} = \frac{1}{tR_{sh}} \quad (13)$$

where ρ is the electrical resistivity, e is the film thickness, I is the applied current and V is the measurement voltage.

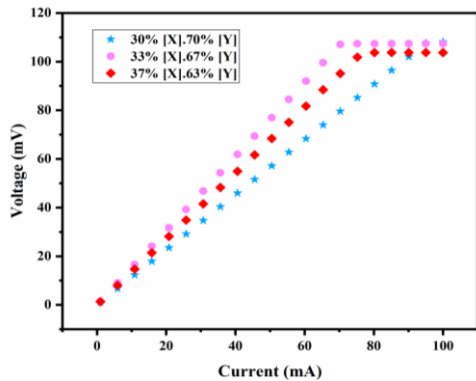


Fig. 11 – Voltage changes in terms of current intensity at various concentrations

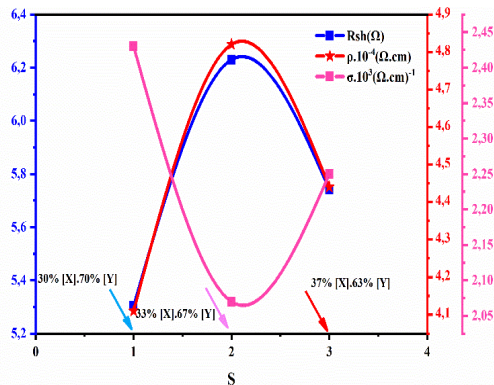


Figure 12 – Sheet resistance, electrical resistivity & electrical conductivity of NiS thin films

4. CONCLUSION

In this work, Nickel sulfide (NiS) thin films were successfully deposited on glass substrates at 250 °C by the spray pyrolysis technique (SPT). The effect of different nickel sulfide precursors on the structural, optical and electrical properties has been studied for each of the following concentrations {30%[X].70%[Y], {33%[X].67%[Y]} and {37%[X].63%[Y]}, The DRX analysis confirms that all polycrystalline samples have a hexagonal structure in the preferred direction (010). The maximum crystallite size (D) was calculated (22.148 nm) for the {30% [X].70% [Y]} ratio sample, On the other hand, the results of the FTIR analysis confirm the presence of the Ni-S bond according to the frequency (626 cm^{-1}) supported by the DRX results. The optical band gap (E_g) values for all nickel sulfide NiS thin film samples are (0.92, 0.87 and 0.88). Moreover The Sheet resistance (R_{sh}) is found in (5.304, 6.230 and 5.741 Ω). This study proved that nickel sulfide (NiS) thin films have good crystallinity and high conductivity. This makes it possible for us to continue working on using thin films in supercapacitors applications.

CONFLICTS OF INTEREST

The authors declare no conflict of interest.

ACKNOWLEDGEMENTS

The authors would like to acknowledge to the Pr. Tibermacine Toufik and Pr. Mohamed Toufik Soltani for the support and help, and Mr. Abderraouf Zidane for his assistance.

FUNDING

The authors did not receive support from any organization for the submitted work. No funding was received to assist with the preparation of this manuscript. No funding was received for conducting this study.

DATA AVAILABILITY STATEMENT

The data presented in this study are available on request from the corresponding author

AUTHOR CONTRIBUTION STATEMENT

All authors contributed to the study conception and design. Material preparation, data collection and analysis were performed by Amira Sbahi, Said Benramache, Chaima Benbrika. The first draft of the manuscript was written by Amira Sbahi and Said Benramache all authors commented on previous versions of the manuscript. All authors read and approved the final manuscript.

REFERENCES

1. A. Gahtar, S. Benramache, L. Fella, A. Zedouri, *Annals of West University of Timisoara – Physics* **63** No 1, 163 (2021).
2. M.M. Gul, K.S. Ahmad, L. Almanqur et al., *J. Appl. Electrochem.* **53**, 257 (2023).
3. A. Gahtar, A. Benali, S. Benramache, C. Zaoucheb, *Chalcogenide Lett.* **19**, 103 (2022).
4. S. Mehta, K. Singh Samra, *J. Phys.: Conf. Ser.* **2267**, 012004 (2022).
5. V. Kumar, D. Sharma, K. Sharma, D. Dwivedi, *Optik* **156**, 43 (2018).
6. A. Gahtar, S. Benramache, A. Ammari, A. Boukhachem, A. Ziouche, *Inorgan. Nano-Metal Chem.* **52**, 112 (2022).
7. M. Venkata-Haritha, C.V.V.M. Gopi, S.-K. Kim, J.-C. Lee, H.-J. Kim, *New Journal of Chemistry* **39**, 1 (2015).
8. R. Boughalmi, R. Rahmani, et al., *Mater. Chem. Phys.* **163**, 99 (2015).
9. S. Suresh, S. Anan, R. Arul, D. Isha, *Chalcogenide Lett.* **13**, 291 (2016).
10. A. Patil, A. Lokhande, P. Shinde, J. Kim, C. Lokhande, *J. Energy Chem.* **27** No 3, 791 (2018).
11. S. Sartale, C. Lokhande, *Mater. Chem. Phys.* **72**, 101 (2001).
12. R.K. Singh, J. Narayan, *Phys. Rev. B: Condens. Matt.* **41**, 8843 (1990).
13. H. Ruan, Y. Li, H. Qiu, M. Wei, *J. Alloy. Compd* **588**, 357 (2014).
14. P. Yang, M. Lu, C.F. Song, G. Zhou, D. Xu, D.R Yuan, *J. Phys. Chem. Solids* **63** No 11, 2047 (2002).
15. V.P. Patil, S. Pawar, M. Chougule, P. Godse, R. Sakhare, S. Sen, P. Joshi, *J. Surf. Eng. Mater. Adv. Technol.* **01**, 35 (2011).
16. A. Gahtar, S. Benramache, C. Zaouche, A. Boukacham, A. Sayah, *Adv. Mater. Sci.* **20**, 36 (2020).
17. T. Srinivasulu, K. Saritha, K.T. Ramakrishna Reddy, *Modern Electronic Materials* **517**, 502 (2017).
18. H. Cheng, X. Zhai, J. Ouyang, L. Zheng, N. Luo, J. Liu, H. Zhu, Y. Wang, L. Hao, K. Wang, *Adv. Ceram.* **12**, 196 (2023).
19. N. Khedmi, M. Ben Rabeh, M. Kanzari, *J. Mater. Sci. Technol.* **30**, 1006 (2014).
20. R.M. Al Jarrah, E.M. Kadhemi, A.O. Alkhatyatt, *Appl. Phys. A* **128**, 527 (2022).
21. S.K. Khaja Muswareena, K. Venkataraoa, S. Cole, *Phys. Chem. Res.* **11**, 241 (2023).
22. U. Farwa, K.S. Ahmad, Z. Hussain, S. Majid, *Surface. Interface.* **12**, 190 (2018).
23. O.O. Balayeva, A.A. Azizov, M.B. Muradov, et al., *Mater. Res. Bull.* **75**, 155 (2016).
24. C. Buchmaier, M. Glanzer, A. Torvisco, P. Poelt, K. Wewerka, B. Kunert, K. Gatterer, *J. Mater. Sci.* **52**, 10898 (2017).
25. K.N. Santhosh, D. Govinda, R.G. Thirumala, *J. Chem. Sci.* **15**, 1 (2017).
26. M. Kristl, B. Dojer, S. Gyergyek, J. Kristl, *Heliyon* **3**, e00273 (2017).
27. A. Ghezelbash, M.B. Sigman, B.A. Korgel, *Nano Lett.* **4**, 537 (2004).
28. S. Benramache, B. Benhaoua, *Superlattice. Microstruct.* **52** No 4, 807 (2012).
29. C. Zaouche, Y. Aoun, S. Benramache, A. Gahtar, *The Scientific Bulletin of Valahia University Materials and Mechanics* **17**, 27 (2019).
30. S. Gedi, V.R.M. Reddy, C. Park, J. Chan-Wook, R.R. KT, *Opt. Mater.* **42**, 468 (2015).
31. A. Gahtar, C. Zaouche, A. Ammari, L. Dahbi, *Chalcogenide Lett.* **20**, 377 (2023).

Синтез тонких плівок надпровідника NiS з високою електропровідністю

A. Sbaihi^{1,2,3}, S. Benramache², C. Benbrika³¹ *Laboratoire des Matériaux Semi-Conducteurs et Métalliques, University of Biskra 07000, Algeria*² *Laboratoire des Matériaux, des Énergies et de l'Environnement, University of Biskra 07000, Algeria*³ *Material Sciences Department, Faculty of Science, University of Biskra 07000, Algeria*

У цій роботі представлені результати досліджень фізичних властивостей наноструктурних тонких плівок сульфідів нікелю (NiS), які були нанесені на нагріті скляні підкладки ($T = 250\text{ }^\circ\text{C}$) за допомогою технології розпилювального піролізу (SPT) з використанням різних концентрацій прекурсорів. Два джерела розчину: гексагідрат нітратів нікелю $\{(\text{Ni}(\text{NO}_3)_2 \cdot 6\text{H}_2\text{O})=\text{X}\}$ і тиосечовина $\{(\text{CS}(\text{NH}_2)_2)=\text{Y}\}$: $\{30\% [\text{X}], 70\% [\text{Y}]\}$, $\{33\% [\text{X}], 67\% [\text{Y}]\}$ та $\{37\% [\text{X}], 63\% [\text{Y}]\}$ із фіксацією інших експериментальних умов. Результати рентгенівського дифракційного аналізу показали, що всі зразки тонких плівок сульфідів нікелю (NiS) є полікристалічними в гексагональній фазі та мають переважну орієнтацію (010). Розмір кристаліту (D) оцінювався за співвідношенням Дебая-Шеррера і становив у діапазоні від 9,915 нм до 22,148 нм. Виникнення зв'язку Ni-S, що відповідає частоті $668,563\text{ cm}^{-1}$, було підтверджено аналізом FTIR. Енергія забороненої зони змінювалася для зразків від 0,87, 0,88 до 0,92 еВ. Опір пластини (R_{sh}) було виміряно за допомогою чотириточкового методу, який використовувався для визначення провідності зразків.

Ключові слова: NiS, Спрей піроліз, Тонка плівка, Рентгенівська дифракція.